Quantum kinetic simulations of nonequilibrium electrons: the G1-G2 scheme

Michael Bonitz, Christopher Makait, Jan-Philip Joost, and Erik Schroedter

Institute for Theoretical Physics and Astrophysics, Kiel University
in collaboration with K. Balzer (Kiel), A. Niggas, and R. A. Wilhelm, TU Vienna

PNP 2024
Oxford, September 2024
pdf at http://www.itap.uni-kiel.de/theo-physik/bonitz/talks.html

Nonequilibrium electron dynamics in warm dense matter

- Experiments on "...ultrafast nonequilibrium collective dynamics in warm dense hydrogen"[1], equilibration of electron and ion temperature
- fs-laser excited warm dense gold[2]: excitation of d-electrons, fluence-dependent reflectivity
- Initial phase of electron compression and heating in indirect and direct drive ICF, validity of radiation-hydrodynamics?
- relaxation of electron momentum distribution, role of e-i and e-e collision
- nonequilibrium density of states, nonequilibrium plasmons and instabilities
- nonequilibrium atomic processes: e.g. impact ionization, Auger ionization, fusion rates

[1] Fäustlin et al., Phys. Rev. Lett. **104**, 125002 (2010).
[2] Blumenstein et al., Phys. Rev. B. **101**, 165140 (2020).
[3] Nagler et al., Nature Phys. **5**, 693 (2009).

Electron dynamics in plasmas with kinetic equations

- **Boltzmann's kinetic equation for the phase space distribution** $f(\mathbf{r}_1, \mathbf{p}_1, t)$

$$\frac{\partial f}{\partial t} + \frac{\mathbf{p}_1}{m} \cdot \nabla f + \mathbf{F}^{\mathrm{tot}} \cdot \frac{\partial f}{\partial \mathbf{p}_1} = \int dp_2 dp_1' dp_2' \, \sigma(p_1, p_2; p_1', p_2') \left\{ f_1' f_2' - f_1 f_2 \right\} \Big|_t = I(p_1, t)$$

- I : two-particle scattering effects, modified by surrounding medium (e.g. screening)
- static screening: Landau; dynamic screening: Balescu-Lenard, strong coupling: T-matrix

$$\sigma^{\mathrm{BL}} \sim \left| \frac{V(p_1 - p_1')}{\epsilon(p_1 - p_1', E_{p_1} - E_{p_1'})} \right|^2 \delta(p_1 + p_2 - p_1' - p_2') \, \delta(E_{p_1} + E_{p_2} - E_{p_1'} - E_{p_2'})$$

- **Problems of the Boltzmann and Balescu equations or Gould-DeWitt scheme:**[1]
  1. strong coupling and dynamical screening not selfconsistent
  2. no total energy conservation (due to Markov limit)
  3. not applicable to femtosecond time scales (no correlation buildup, no plasmon dynamics)
- **Are these effects important? Are they measurable?**

[1] for details, see M. Bonitz, *Quantum Kinetic Theory*, 2nd ed., Springer 2016

Plasma interaction with quantum materials[2]

- Experiments with highly charged ions at TU Vienna (R. Wilhelm)
- Xe^{40+} ion penetrates monolayers of graphene and MoS_2
- ultrafast emission of slow electrons into vacuum: ca. 80 per ion, 6 times more electrons released from graphene $\Rightarrow$ sensitive local probe of electronic properties
- theoretical explanation?
  suitable approaches?

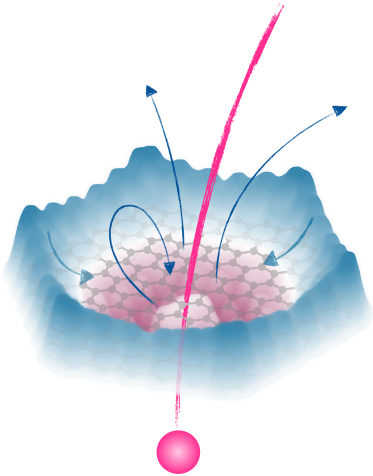

[2] A. Niggas *et al.*, Phys. Rev. Lett. **129**, 086802 (2022), Editors' Choice

Time-dependent Schrödinger equation. Scaling bottleneck

- time-dependent many-electron Hamiltonian

$$H(t) = \underbrace{\sum_{i=1}^{N} h(\boldsymbol{r}_i, t)}_{\text{one-body operators}} + \underbrace{\frac{1}{2}\sum_{i\neq j}^{N} W(\boldsymbol{r}_i, \boldsymbol{r}_j)}_{\textbf{pair-wise}\ \text{interactions}}$$

- time-dependent Schrödinger equation (TDSE)

$$i\partial_t \Psi(\boldsymbol{r}_i, \ldots, \boldsymbol{r}_N; t) = H(t)\Psi(\boldsymbol{r}_i, \ldots, \boldsymbol{r}_N; t) \quad \overset{\text{direct solution}}{\cancel{\longrightarrow}} \quad \Psi(\boldsymbol{r}_i, \ldots, \boldsymbol{r}_N; t)$$

exponential scaling of numerical effort

- **solutions to overcome exponential scaling:**
  1. approximations to TDSE: TD-RASCI, TD-CASSCF, truncated CC, TD-R-matrix etc. D. Hochstuhl and M. Bonitz, PRA (2012) and EJP-ST (2014)
  2. propagation of simpler observables: density (TDDFT), distribution function (Kinetic theory), correlation functions etc.

Scaling of quantum many-body methods

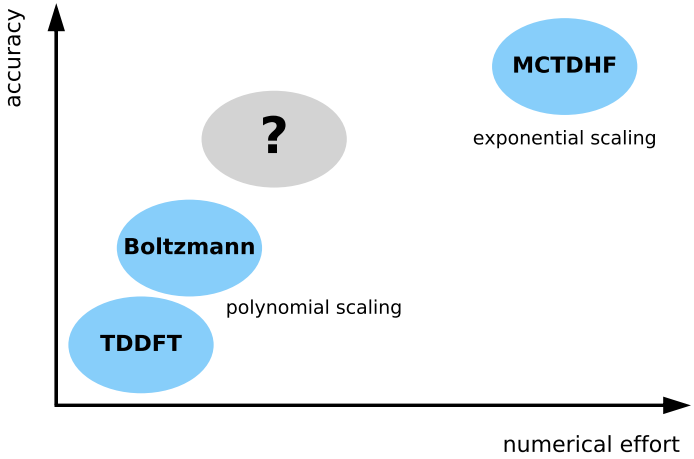

*MCTDHF and other wavefunction-based methods

? Can one achieve sufficient accuracy (including e-e collisions) at non-exponential cost?

Nonequilibrium Green Functions (NEGF)

2nd quantization

- Fock space $\mathcal{F} \ni |n_1, n_2 \ldots\rangle$, $\quad \mathcal{F} = \bigoplus_{N_0 \in \mathbb{N}} \mathcal{F}^{N_0}$, $\quad \mathcal{F}^{N_0} \subset \mathcal{H}^{N_0}$
- $\hat{c}_i, \hat{c}_i^\dagger$ creates/annihilates a particle in single-particle orbital ϕ_i
- spin accounted for by canonical (anti-)commutator relations
  $\left[\hat{c}_i^{(\dagger)}, \hat{c}_j^{(\dagger)}\right]_\mp = 0, \quad \left[\hat{c}_i, \hat{c}_j^\dagger\right]_\mp = \delta_{i,j}$
- Hamiltonian: $\hat{H}(t) = \underbrace{\sum_{k,m} h^0_{km} \hat{c}_k^\dagger \hat{c}_m}_{\hat{H}_0} + \underbrace{\frac{1}{2} \sum_{k,l,m,n} w_{klmn}\, \hat{c}_k^\dagger \hat{c}_l^\dagger \hat{c}_n \hat{c}_m}_{\hat{W}} + \hat{F}(t)$

Particle interaction w_{klmn}

- Coulomb interaction
- electronic correlations

Time-dependent excitation $\hat{F}(t)$

- single-particle type
- em field, quench, particles

Nonequilibrium Green Functions (NEGF)

two times $z, z' \in \mathcal{C}$ ("Keldysh contour"), arbitrary one-particle basis $|\phi_i\rangle$

$$\boxed{G_{ij}(z,z') = \frac{\mathrm{i}}{\hbar}\left\langle \hat{T}_{\mathcal{C}}\hat{c}_i(z)\hat{c}_j^\dagger(z')\right\rangle}$$

average with $\hat{\rho}_N$

pure or mixed state

Keldysh–Kadanoff–Baym equations (KBE) on $\mathcal{C}$ (2×2 matrix):

$$\sum_k \left\{\mathrm{i}\hbar\frac{\partial}{\partial z}\delta_{ik} - h_{ik}(z)\right\} G_{kj}(z,z') = \delta_{\mathcal{C}}(z,z')\delta_{ij} - \mathrm{i}\hbar\sum_{klm}\int_{\mathcal{C}} \mathrm{d}\bar{z}\, w_{iklm}(z^+,\bar{z})G^{(2)}_{lmjk}(z,\bar{z};z',\bar{z}^+)$$

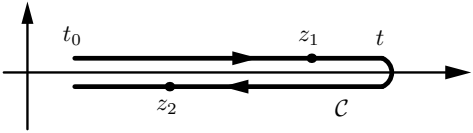

KBE: first equation of Martin–Schwinger hierarchy for $G, G^{(2)} \dots G^{(n)}$

- $\int_{\mathcal{C}} wG^{(2)} \to \int_{\mathcal{C}} \Sigma G$, Selfenergy
- Nonequilibrium Diagram technique
  Example: Hartree–Fock + Second Born selfenergy

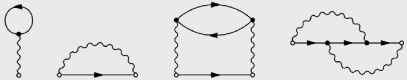

Real-Time Keldysh–Kadanoff–Baym Equations (KBE)

- Correlation functions $G^{\gtrless}$ obey real-time KBE

$$\sum_l \left[\mathrm{i}\hbar \frac{\mathrm{d}}{\mathrm{d}t} \delta_{i,l} - h^{\mathrm{eff}}_{il}(t) \right] G^{>}_{lj}(t,t') = I^{(1),>}_{ij}(t,t') \,,$$

$$\sum_l G^{<}_{il}(t,t') \left[-\mathrm{i}\hbar \frac{\overleftarrow{\mathrm{d}}}{\mathrm{d}t'} \delta_{l,j} - h^{\mathrm{eff}}_{lj}(t') \right] = I^{(2),<}_{ij}(t,t') \,,$$

with the effective single-particle **Hartree–Fock Hamiltonian**

$$h^{\mathrm{eff}}_{ij}(t) = h^{0}_{ij} \pm \mathrm{i}\hbar \sum_{kl} w^{\pm}_{ikjl} G^{<}_{lk}(t)$$

and the collision integrals

$$I^{(1),>}_{ij}(t,t') := \sum_l \int_{t_\mathrm{s}}^{\infty} \mathrm{d}\bar{t} \left\{ \Sigma^{\mathrm{R}}_{il}(t,\bar{t}) G^{>}_{lj}(\bar{t},t') + \Sigma^{>}_{il}(t,\bar{t}) G^{\mathrm{A}}_{lj}(\bar{t},t') \right\} ,$$

$$I^{(2),<}_{ij}(t,t') := \sum_l \int_{t_\mathrm{s}}^{\infty} \mathrm{d}\bar{t} \left\{ G^{\mathrm{R}}_{il}(t,\bar{t}) \Sigma^{<}_{lj}(\bar{t},t') + G^{<}_{il}(t,\bar{t}) \Sigma^{\mathrm{A}}_{lj}(\bar{t},t') \right\} .$$

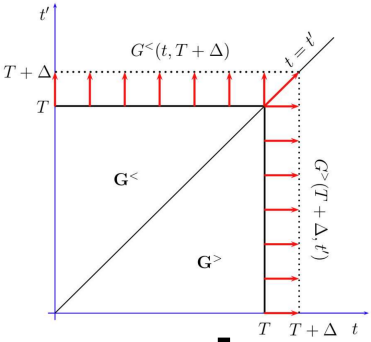

$$\mathcal{O}(N_\mathrm{t}^3)$$

- two-time structure contains spectral information
- numerically demanding due to cubic scaling with number of time steps N_t

Selfenergy Approximations[3]

Choice depends on coupling strength, density (filling)

Hartree–Fock (HF, mean field): $\sim w^1$

Second Born (2B): $\sim w^2$

GW: ∞ bubble summation, dynamical screening effects

particle-particle T-matrix (TPP): ∞ ladder sum in pp channel

particle-hole T-matrix (TPH/TEH): ∞ ladder sum in ph channel

3rd order approx. (TOA): $\sim w^3$

dynamically screened ladder (DSL)*: $\sim \mathrm{2B} + GW + \mathrm{TPP} + \mathrm{TPH}$

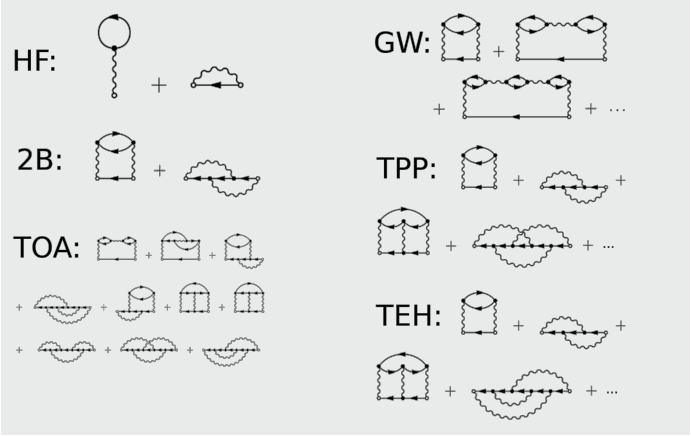

[3]Conserving approximations, nonequilibrium $\Sigma(t, t')$, applies for ultra-short to long times
Review: Schlünzen *et al.*, J. Phys. Cond. Matt. **32**, 103001 (2020); *Joost *et al.*, PRB (2022)

Testing various selfenergies: the Hubbard model

- Simple, but versatile model for strongly correlated solid state systems, 2D materials
- Suitable for single band, small bandwidth; atoms in optical lattices

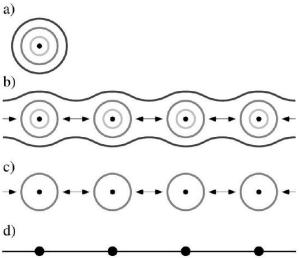

$\Rightarrow$

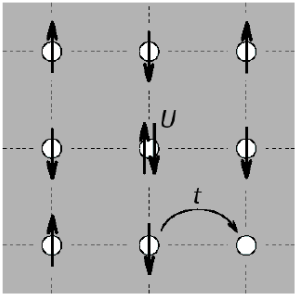

$$\hat{H}(t) = J \sum_{ij,\,\alpha} h_{ij}\, \hat{c}^{\dagger}_{i\alpha} \hat{c}_{j\alpha} + U \sum_i \hat{c}^{\dagger}_{i\uparrow} \hat{c}_{i\uparrow} \hat{c}^{\dagger}_{i\downarrow} \hat{c}_{i\downarrow} + \sum_{ij,\alpha\beta} f_{ij,\alpha\beta}(t)\, \hat{c}^{\dagger}_{i\alpha} \hat{c}_{j\beta}$$

$h_{ij} = -\delta_{\langle i,\,j\rangle}$ nearest neighbor hopping, on-site repulsion ($U > 0$) or attraction ($U < 0$),

- f : external single-particle potential: e.g. potential quench, laser field, ion impact
- parameters from electronic structure calculations (DFT) or experiment
- can be systematically improved: extended Hubbard and PPP model, multiple bands

Benchmarks of NEGF against DMRG (1D)[5]

Initial state:
charge density wave

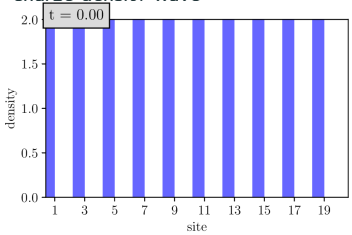

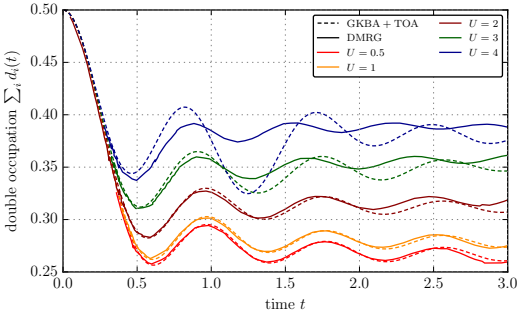

- sensitive observable: total double occupation
- good quality transients NEGF up to $U \simeq$ bandwidth
- accurate long-time behavior of GKBA+T-matrix (not shown)
- performance of different selfenergies vs. coupling and filling[4]

[4] N. Schlünzen, S. Hermanns, M. Scharnke, and M. Bonitz, J. Phys.: Cond. Matt. **32** (10), 103001 (2020)
[5] N. Schlünzen, J.-P. Joost, F. Heidrich-Meisner, and M. Bonitz, Phys. Rev. B **95**, 165139 (2017)

NEGF vs. experiment: LDOS of graphene nanoribbons: Bulk and End

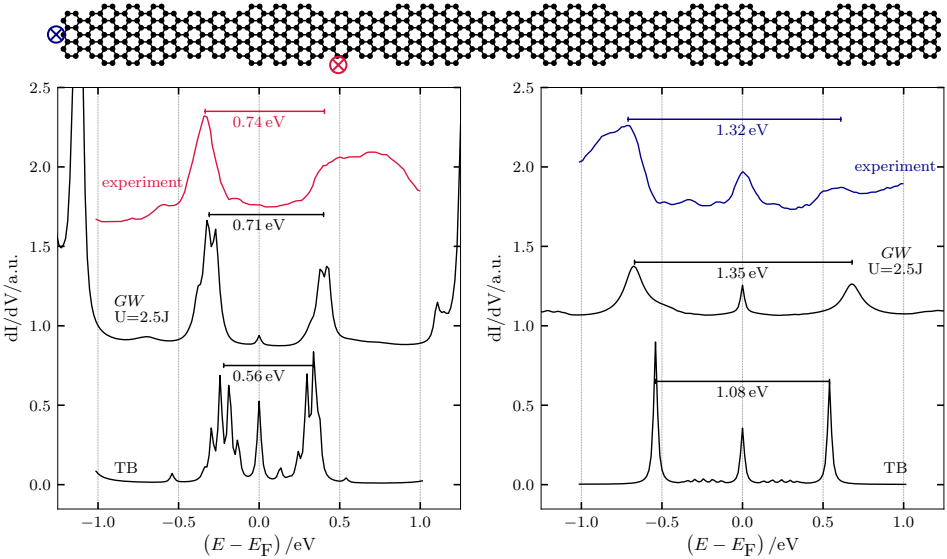

Failure of tight binding and Hartree-Fock. Excellent agreement of NEGF-GW: electronic correlations crucial

Experiments: Rizzo *et al.* Nature, **560**, 204 (2018), NEGF simulations: Joost *et al.* Nano Lett. **19**, 9045 (2019)

Acceleration: Generalized Kadanoff–Baym Ansatz (GKBA)[6]

- full propagation on the time diagonal ($I := I^{(1),<}$):

$$\mathrm{i}\hbar\frac{\mathrm{d}}{\mathrm{d}t}G^{<}_{ij}(t) = \left[h^{\mathrm{HF}}, G^{<}\right]_{ij}(t) + \left[I + I^{\dagger}\right]_{ij}(t)$$

- reconstruct off-diagonal NEGF from time diagonal:

$$G^{\gtrless}_{ij}(t,t') = \pm\left[G^{\mathsf{R}}_{ik}(t,t')\rho^{\gtrless}_{kj}(t') - \rho^{\gtrless}_{ik}(t)G^{\mathsf{A}}_{kj}(t,t')\right]$$

with $\rho^{\gtrless}_{ij}(t) = \pm\mathrm{i}\hbar G^{\gtrless}_{ij}(t,t)$

- HF-GKBA: use Hartree–Fock propagators for $G^{\mathsf{R/A}}_{ij}$

$$G^{\mathsf{R/A}}_{ij}(t,t') = \mp\mathrm{i}\Theta_{\mathcal{C}}\left(\pm[t-t']\right)\exp\left(-\frac{\mathrm{i}}{\hbar}\int_{t'}^{t}\mathrm{d}\bar{t}\, h_{\mathsf{HF}}(\bar{t})\right)\Bigg|_{ij}$$

- conserves total energy

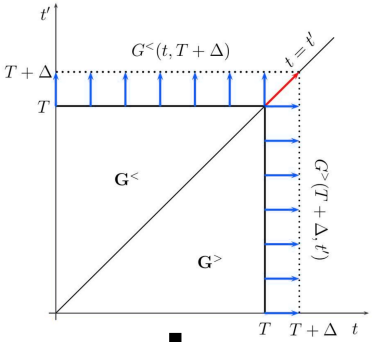

$$\mathcal{O}(N_{\mathsf{t}}^2)$$

[6] P. Lipavský, V. Špička, and B. Velický, Phys. Rev. B **34**, 6933 (1986);
K. Balzer and M. Bonitz, Lecture Notes in Physics **867** (2013)

Time-linear NEGF simulations: the G1–G2 Scheme[7]

- full propagation on the time diagonal as for ordinary HF-GKBA:

$$\mathrm{i}\hbar\frac{\mathrm{d}}{\mathrm{d}t}G^{<}_{ij}(t) = \left[h^{\mathrm{HF}}, G^{<}\right]_{ij}(t) + \left[I + I^{\dagger}\right]_{ij}(t)$$

- but collision integral defined by correlated two-particle Green function

$$I_{ij}(t) = \pm\mathrm{i}\hbar\sum_{klp} w_{iklp}(t)\mathcal{G}_{lpjk}(t)$$

$$\mathcal{O}(N_{\mathrm{t}}^{1})$$

- which obeys an ordinary differential equation

$$\mathrm{i}\hbar\frac{\mathrm{d}}{\mathrm{d}t}\mathcal{G}_{ijkl}(t) = \left[h^{(2),\mathrm{HF}}, \mathcal{G}\right]_{ijkl}(t) + \Psi^{\pm}_{ijkl}(t)$$

- the initial values

$$G^{0,<}_{ij} = \pm\frac{1}{\mathrm{i}\hbar}n_{ij}(t_0) =: \pm\frac{1}{\mathrm{i}\hbar}n^{0}_{ij}\,,$$

$$\mathcal{G}^{0}_{ijkl} = \frac{1}{(\mathrm{i}\hbar)^2}\left\{n^{0}_{ijkl} - n^{0}_{ik}n^{0}_{jl} \mp n^{0}_{il}n^{0}_{jk}\right\}\,,$$

determine the density and the pair correlations existing in the system at the initial time $t = t_0$

[7] N. Schlünzen, J.-P. Joost, and M. Bonitz, Phys. Rev. Lett. **124**, 076601 (2020)

The G1–G2 Scheme: beyond 2nd Born selfenergy

- other selfenergy approximations can be reformulated in the G1–G2 scheme in similar fashion:[8]

$$\mathrm{i}\hbar\frac{\mathrm{d}}{\mathrm{d}t}\mathcal{G}_{ijkl}(t) = \left[h^{(2),\mathsf{HF}}(t), \mathcal{G}(t)\right]_{ijkl} + \Psi^{\pm}_{ijkl}(t) + \underbrace{L_{ijkl}(t)}_{\mathsf{TPP}} + \underbrace{P_{ijkl}(t)}_{GW} \pm \underbrace{P_{jikl}(t)}_{\mathsf{TPH}}$$

$$L_{ijkl} := \sum_{pq}\left\{\mathfrak{h}^{L}_{ijpq}\mathcal{G}_{pqkl} - \mathcal{G}_{ijpq}\left[\mathfrak{h}^{L}_{klpq}\right]^{*}\right\}, \qquad \mathfrak{h}^{L}_{ijkl} := (\mathrm{i}\hbar)^2\sum_{pq}\left[\mathcal{G}^{\mathsf{H},>}_{ijpq} - \mathcal{G}^{\mathsf{H},<}_{ijpq}\right] w_{pqkl}\,,$$

$$P_{ijkl} := \sum_{pq}\left\{\mathfrak{h}^{\Pi}_{qjpl}\mathcal{G}_{piqk} - \mathcal{G}_{qjpl}\left[\mathfrak{h}^{\Pi}_{qkpi}\right]^{*}\right\}, \qquad \mathfrak{h}^{\Pi}_{ijkl} := \pm(\mathrm{i}\hbar)^2\sum_{pq} w^{\pm}_{qipk}\left[\mathcal{G}^{\mathsf{F},>}_{jplq} - \mathcal{G}^{\mathsf{F},<}_{jplq}\right]$$

and the Hartree/Fock (H/F) two-particle Green functions

$$\mathcal{G}^{\mathsf{H},\gtrless}_{ijkl}(t) := G^{\gtrless}_{ik}(t,t)G^{\gtrless}_{jl}(t,t)\,, \qquad \mathcal{G}^{\mathsf{F},\gtrless}_{ijkl}(t) := G^{\gtrless}_{il}(t,t)G^{\lessgtr}_{jk}(t,t)$$

- include TPP, GW and TPH terms simultaneously: dynamically-screened-ladder (DSL) approximation. Conserving, applicable to short times. no explicit DSL selfenergy is known.[9]
- nonequilibrium generalization of ground state result (Bethe-Salpeter equation)

[8] J.-P. Joost, N. Schlünzen, and M. Bonitz, PRB **101**, 245101 (2020), Joost et al., PRB **105**, 165155 (2022);

[9] J.-P. Joost, PhD thesis, Kiel University 2023

Non-Markovian NEGF simulations of ion and electron stopping

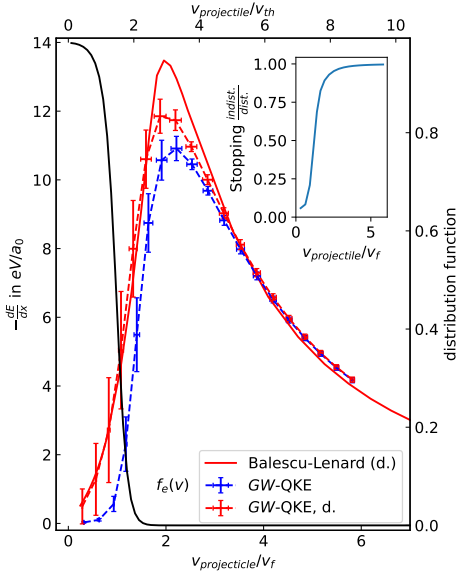

- non-Markovian GKBA-GW simulations (scaling with N_t quadratic for SOA, qubic for GW)
- **Equilibrium plasma, low beam density** mono-energetic projectile
- $r_s = 1$, $\Theta = 0.3$
- significant non-Markovian effects
- Pauli blocking crucial for electron stopping at $\Theta \lesssim 1$

C. Makait, J. Vorberger, and M. Bonitz, to be published

G1–G2–GW stopping simulations. Time-dependent distributions

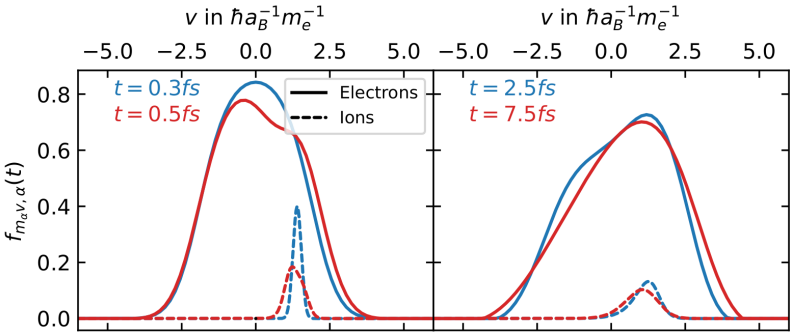

quasi-1D electron-ion plasma, $r_s = 0.5$, $\Theta = 0.81$, ion impact at $t = 0.3$fs

finite projectile density, nonlinear dynamics of distributions

G1–G2: time-linear simulations, DSL and long simulations possible

M. Bonitz *et al.*, Phys. Plasmas (2024), arxiv: 2405.10627

1D model: C. Makait *et al.*, Contrib. Plasma Phys. **63**, e202300008 (2023)

G1–G2–GW stopping simulations. Time-dependent observables

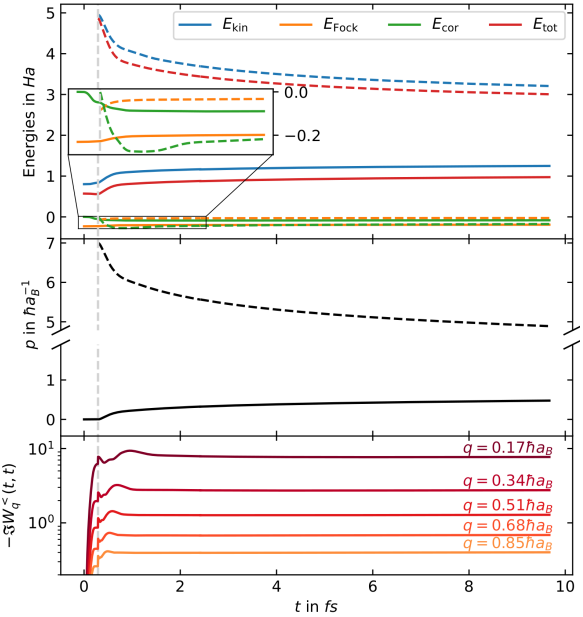

quasi-1D electron-ion plasma $r_s = 0.5$, $\Theta = 0.81$, ion impact at $t = 0.3$fs

full lines: electrons, dashes: ions (beam)

- Top: energy contributions per particle
- Middle: momentum per particle
- bottom: plasmon occupation

M. Bonitz *et al.*, Phys. Plasmas (2024), arxiv: 2405.10627

NEGF-Ehrenfest simulations of ion stopping in quantum materials

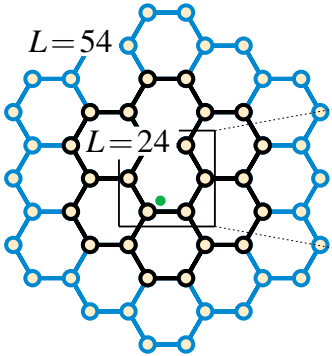

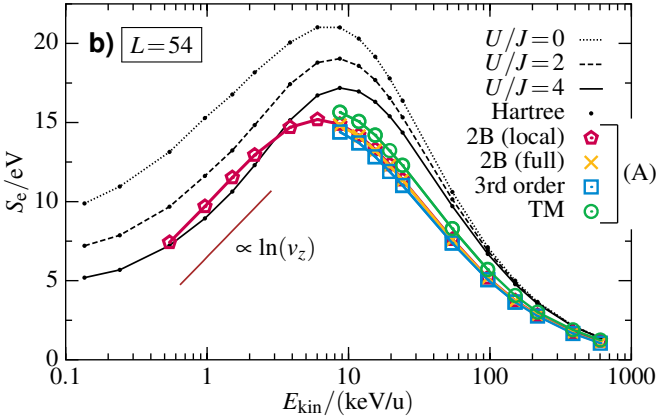

Left: finite honeycomb cluster and impact point of ion (green). Right: Ion energy loss S_e vs. impact energy. Black lines: Hartree approximation for e-e interaction. Colors: different approximations for the correlation selfenergy. Electron correlations generally reduce stopping, except for low impact energy.
From: K. Balzer, N. Schlünzen, and M. Bonitz PRB **94**, 245118 (2016)

NEGF-embedding scheme for charge transfer from graphene nanoflake to impacting high-Z ion

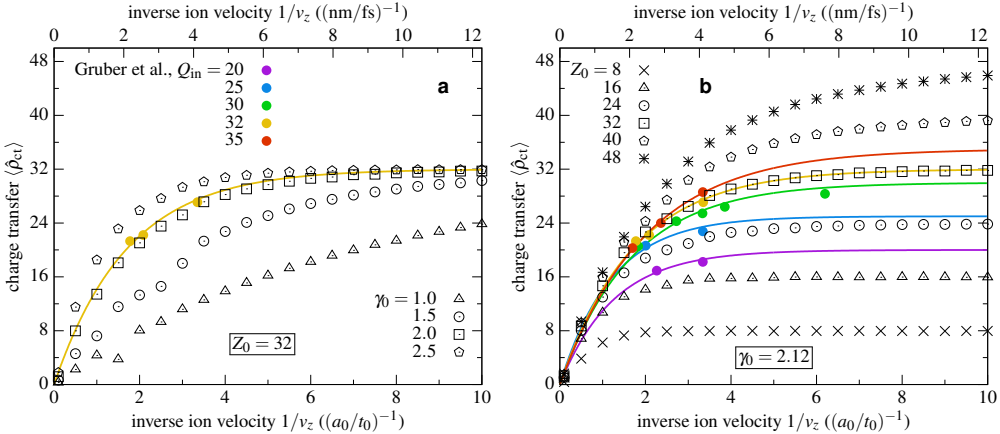

NEGF-embedding selfenergy scheme for resonant charge transfer, $L = 24$. Exp. data from Gruber et al. Nat. Commun. 2016, **7**(1), 13948. Single adjustable parameter γ_0 works for all charges. Figure from Balzer and Bonitz, Contrib. Plasma Phys. **62** (2) e202100041 (2022)

Ion induced secondary electron emission: graphene vs. MoS_2

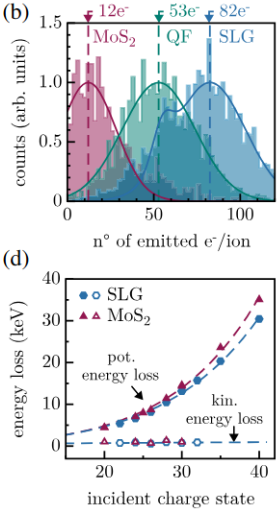

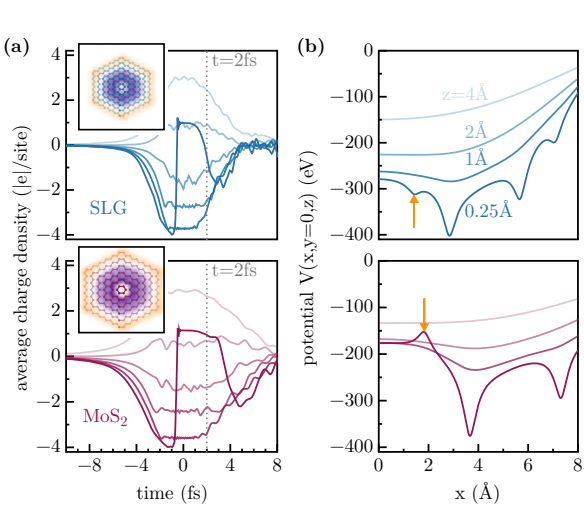

Left: Experiment. **Right**: NEGF simulations of time-resolved radial electron density and induced electrostatic potential, $V(\mathbf{r}, t)$ at $t = 2$ fs, versus radial coordinate x. 113 keV Xe^{32+} ions passing through the center of a 216-site cluster. Niggas. *et al.*, Phys. Rev. Lett. **129**, 086802 (2022)

Energy spectrum without ion and directly before impact

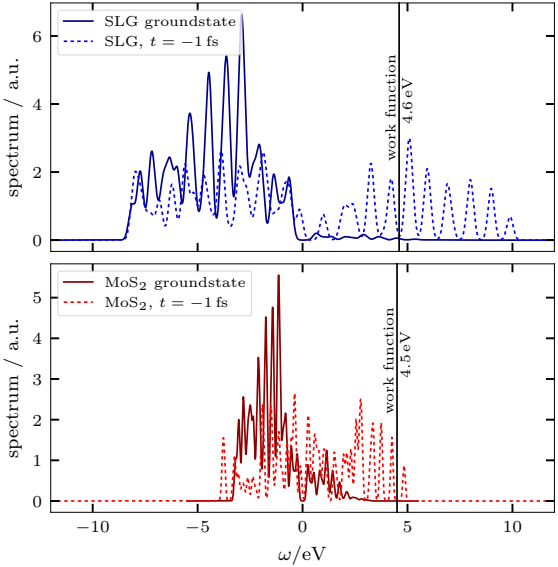

G1–G2 scheme (SOA selfenergy): 113 keV Xe^{32+} ion, graphene: $J = 2.8eV$, $U/J = 1.6$, $a_L = 1.42$Å
MoS_2: $J = 1.1eV$, $U/J = 4.0$, $a_L = 1.83$Å, Niggas. et al., Phys. Rev. Lett. **129**, 086802 (2022)

Summary and Outlook

- NEGF simulations are the most accurate approach to quantum many-body systems out of equilibrium on all time scales
- advanced selfenergies capture key electronic excitation processes, strong coupling and dynamical screening, well tested for lattice models (accurate with DFT input parameters)
- G1–G2 calculations allow for long and efficient simulations (linear in time)[10]
- applied to stopping power in quantum materials and dense plasmas
- ion neutralization via resonant charge transfer modeled using a NEGF embedding selfenergy approach.
- current limitation: main memory. Can be solved via a novel quantum fluctuations approach, e.g. Schroedter *et al.*, phys. stat. sol. (b) 2300564 (2024) and with a G1–G2 embedding scheme, see Balzer *et al.*, PRB **107**, 155141 (2023)

[10] N. Schlünzen, J.-P. Joost and M. Bonitz, Phys. Rev. Lett. **124**, 076601 (2020)
J.-P. Joost, N. Schlünzen, and M. Bonitz, Phys. Rev. B **101**, 245101 (2020)
J.-P. Joost, N. Schlünzen, H. Ohldag, M. Bonitz, F. Lackner, and I. Brezinova, Phys. Rev. B **105**, 165155 (2022)

Towards first principles-based simulations in WDM[11]

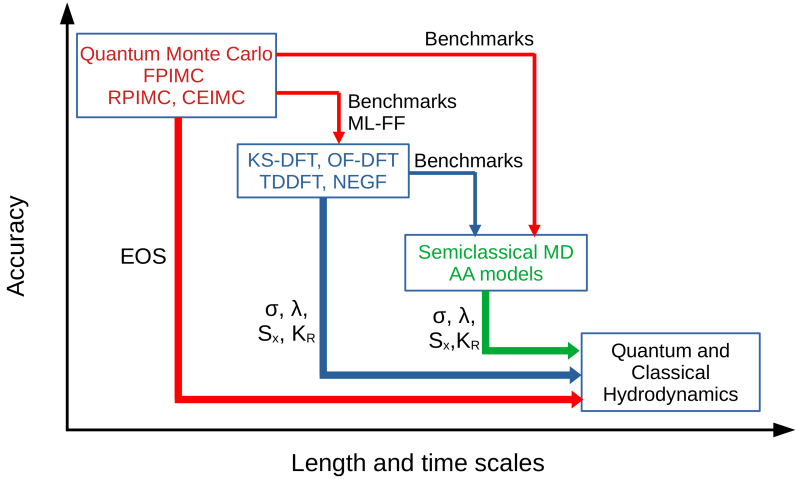

- To cover all length and time scales, a combination of methods is necessary.
- basis: first principles-based benchmarks for test cases

[11] Hydrogen review, M. Bonitz *et al.*, Phys. Plasmas 2024, arxiv: 2405.10627

Scaling of nonequilibrium quantum many-body methods revisited

G1–G2 scheme allows for highly efficient accurate (selfconsistently including strong correlations and dynamical screening), long and stable quantum dynamics, for systems of any geometry and time scale

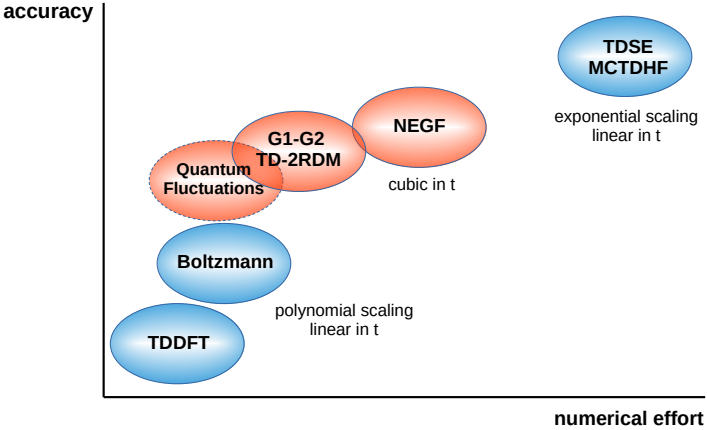

Extensions to complex condensed matter systems: combination with TDDFT.

Extension to larger length and time scales: combination with AA-models and (Q)hydrodynamics